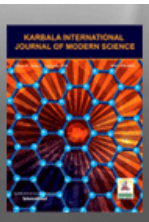

Karbala International Journal of Modern Science

Volume 8 | Issue 4 Article 8

Magnéli Phase Titanium Sub-Oxide Production using a Hydrothermal Process

Mohanad Q. Fahem
Department of Physics, College of Science, University of Baghdad, Baghdad

Thamir A.A. Hassan
Al-Karkh University of Science, Baghdad, president@kus.edu.iq

Recommended Citation

Fahem, Mohanad Q. and Hassan, Thamir A.A. (2022) "Magnéli Phase Titanium Sub-Oxide Production using a Hydrothermal Process," *Karbala International Journal of Modern Science*: Vol. 8 : Iss. 4 , Article 8.
Available at: https://doi.org/10.33640/2405-609X.3265

Magnéli Phase Titanium Sub-Oxide Production using a Hydrothermal Process

Abstract

One gram of TiO2 nanoparticles, size of 30-50 nm and 20 ml of 3M of NaOH as the suspension were utilized in a hy-drothermal process using three homemade reactors of different surface areas but of the same capacity to synthesise tita-nium sub-oxide Ti6O11. X-ray diffraction, Raman spectroscopy, and field-emission scanning electron microscopy (FE-SEM) were employed to characterise the samples. When the temperature was raised to 363 K (90 °C) for 6 h and the surface area changed, X-ray diffraction revealed the development of sub-oxide titanium (Ti6O11) with a triclinic Magnéli phase from TiO2 nanoparticles. FE-SEM revealed consistent hierarchical structures with grass-like planar ge-ometries. In titanium, a new phase has been discovered.

Keywords

Magnéli, titanium sub-oxide Ti6O11, Hydrothermal, hierarchical structure, Raman

RESEARCH PAPER

Magnéli Phase Titanium Sub-Oxide Production Using a Hydrothermal Process

Mohanad Q. Fahem [a,*], Thamir A.A. Hassan [b]

[a] Department of Physics, College of Science, University of Baghdad, Baghdad, Iraq
[b] Alkarkh University of Science / Baghdad-Iraq, Baghdad, Iraq

Abstract

One gram of TiO_2 nanoparticles, size of 30−50 nm and 20 mL of 3M of NaOH as the suspension were utilized in a hydrothermal process using three homemade reactors of different surface areas but of the same capacity to synthesise titanium sub-oxide Ti_6O_{11}. X-ray diffraction, Raman spectroscopy, and field-emission scanning electron microscopy (FE-SEM) were employed to characterise the samples. When the temperature was raised to 363 K (90 °C) for 6 h and the surface area changed, X-ray diffraction revealed the development of sub-oxide titanium (Ti_6O_{11}) with a triclinic Magnéli phase from TiO_2 nanoparticles. FE-SEM revealed consistent hierarchical structures with grass-like planar geometries. In titanium, a new phase has been discovered.

Keywords: Magnéli, Titanium sub-oxide Ti_6O_{11}, Hydrothermal, Hierarchical structure, Raman

1. Introduction

Producing partially oxidised titanium dioxide by the hydrothermal method has become a topic of interest in recent years. The method is used in various applications due to the unique features of the nanostructures produced.

In the 1950s, Magnéli solved the structure of Ti_nO_{2n-1}. With the exception that sharing occurs in each octahedron due to Ti reduction and the resulting oxygen vacancies in Ti_nO_{2n-1}, which is identical to the edge-shared TiO_6 octahedra chain structure [1,2]. The titanium suboxides known as Magnéli phases have the general formula Ti_nO_{2n-1} (n is an integer between 4 and 10) [3,4].

Ti_nO_{2n-1} is a highly conductive oxide with unique physical, chemical, and optical properties. Due to its small bandgap, it could be used in photocatalysis, photovoltaics, fuel cells, data storage, and energy conversion devices [5,6]. Various methods, including RF induction thermal plasma, laser chemical vapor deposition, photo electrochemical water splitting (preparation requires 1000 °C) and hydrothermal method, are used to synthesise Magnéli phases. The titanium−oxygen system is used in several applications and plays an important part in the research of a material's non-stoichiometry owing to its remarkable conductivity and extreme visible light absorptivity [7−10]. A Magnéli phase has been used as a counter electrode in solar cells and has been proven to have a higher short-circuit current density than that of Pt. The phase is also corrosion-resistant [11,12].

The physical and chemical properties of TiO_2 are influenced by crystal phase, particle size, and particle shape [13−15]. TiO_2 occurs in three crystalline phases: rutile, brookite, and anatase. The rutile phase is thermodynamically stable, whereas brookite and anatase are not [16]. Rutile TiO_2 is also more active in photochemical applications than anatase TiO_2 according to various observations in the literature [11,17].

Controlling the crystallization, size, and shape of nanostructured TiO_2 are critical for producing materials with desirable properties [18,19].

Although a direct correlation between surface and physicochemical properties is not always

Received 8 May 2022; revised 1 August 2022; accepted 2 August 2022.
Available online 10 November 2022

* Corresponding author.
E-mail addresses: mohand.qasem@gmail.com (M.Q. Fahem), president@kus.edu.iq (T.A.A. Hassan).

https://doi.org/10.33640/2405-609X.3265

achievable, crystal structure, surface condition, and size distribution have all been found to influence TiO_2 activity [20,21].

Raman spectroscopy is a powerful technique for exploring the structural characteristics of nanoparticles. It provides critical information on surface morphology and the impacts of the finite size of nanoparticles. Particle size reduction, causing the rise in the surface to volume ratio, can be detected from changes in Raman spectra, including the appearance of new bands and the vanishing or broadening of existing bands. Campbell and Fauchet showed that grain size effects cause substantial changes and broadening of the Raman spectrum [22,23].

2. Experimental

2.1. Materials and methods

Rutile titanium dioxide Nano TiO_2 Powder (Purchased from Hongwu international Group) with purity 99.983%; Particle size 30–50 nm has high stable corrosion resistance. NaOH was purchased from Sigma Aldrich with a purity of 98%.

2.2. Setup the different autoclave reactors

Three stainless steel reactors A, B, and C of 100 mL capacity with dimensions [diameter: height]: A (55 mm: 130 mm), B (65 mm: 100 mm), and C (75 mm: 80 mm) as shown in Fig. 1 were designed and fabricated in our laboratory.

Each reactor consists of an inner Teflon autoclave positioned inside a stainless steel (Type 304) cylinder that can be tightly closed with a screwed cover. The cylinder acts as a furnace because it is surrounded externally by a 3000 W heater and is supplied with a thermocouple for temperature control. The stainless steel autoclave is the basic component of the reactors that contain a Teflon autoclave and upper and lower gasket seals. All are surrounded by a heater.

2.3. Preparation of Ti_6O_{11} by hydrothermal method

Figure 2 shows the steps of the hydrothermal process; One gram of rutile TiO_2 nanoparticles (NPs) was added to 20 mL of 3 M NaOH at room temperature. The mixture was stirred continuously until its color changed to white, a process that required 20 min at the most. The white suspension (20 mL) was poured inside each autoclave reactor and heated to a temperature of 363 K for 6 h to prepare the nano-titanium sub-oxide Magnéli phase.

The reaction products in the autoclave reactors were washed several times with ethanol and distilled water, dried for 30 min, and filtered by a Büchner funnel using filter paper (pore size = 200 nm). Finally, the product was heated at 523 K for 1 h to increase homogeneity and remove any residual organic materials.

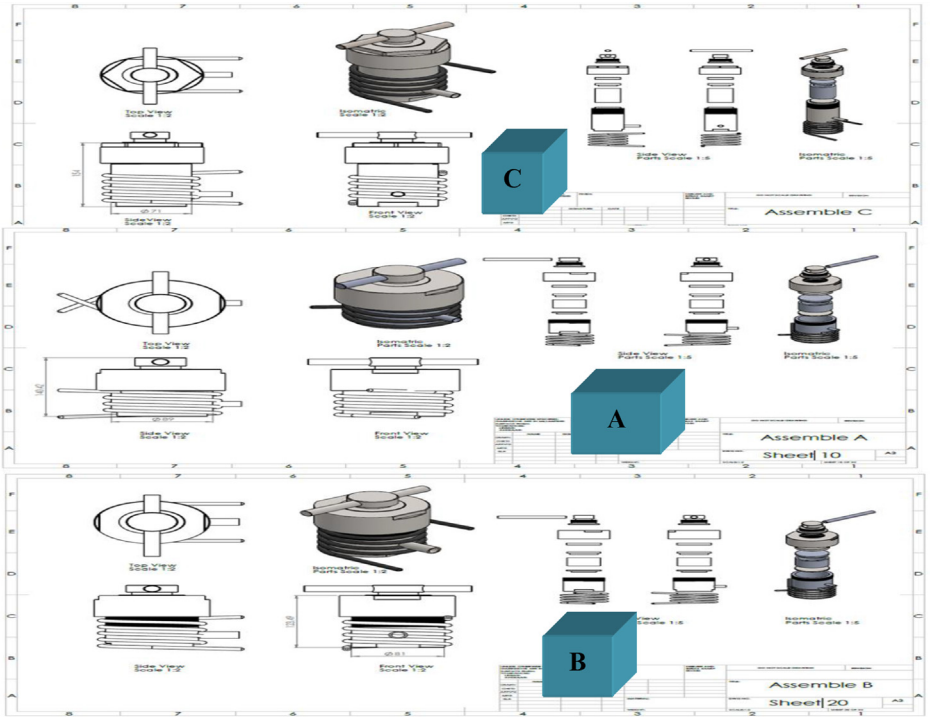

Fig. 1. Schematic diagram showing the dimensions of the three autoclave reactors.

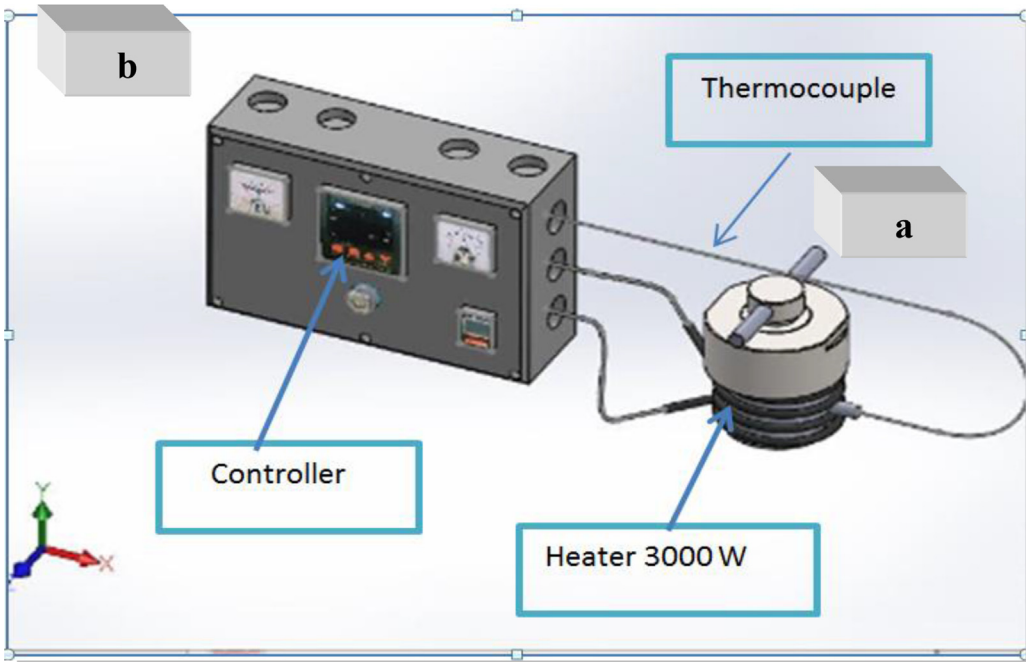

Fig. 2. Hydrothermal system a: controller device. b: Autoclave Reactor Chamber.

The structural properties of the prepared samples were studied by X-ray diffraction (XRD) (Analytical X' Pert Pro, United Kingdom) and Raman spectroscopy (HORIBA XploRA PLUS, Japan). In addition, the surface morphology of the samples was studied using a field-emission scanning electron microscope (EBSD Instrument: ZEISS SIGMA VP, Germany).

3. Results and discussion

Figure 3 shows the XRD patterns of the products from the three reactors, A, B, and C. The patterns are

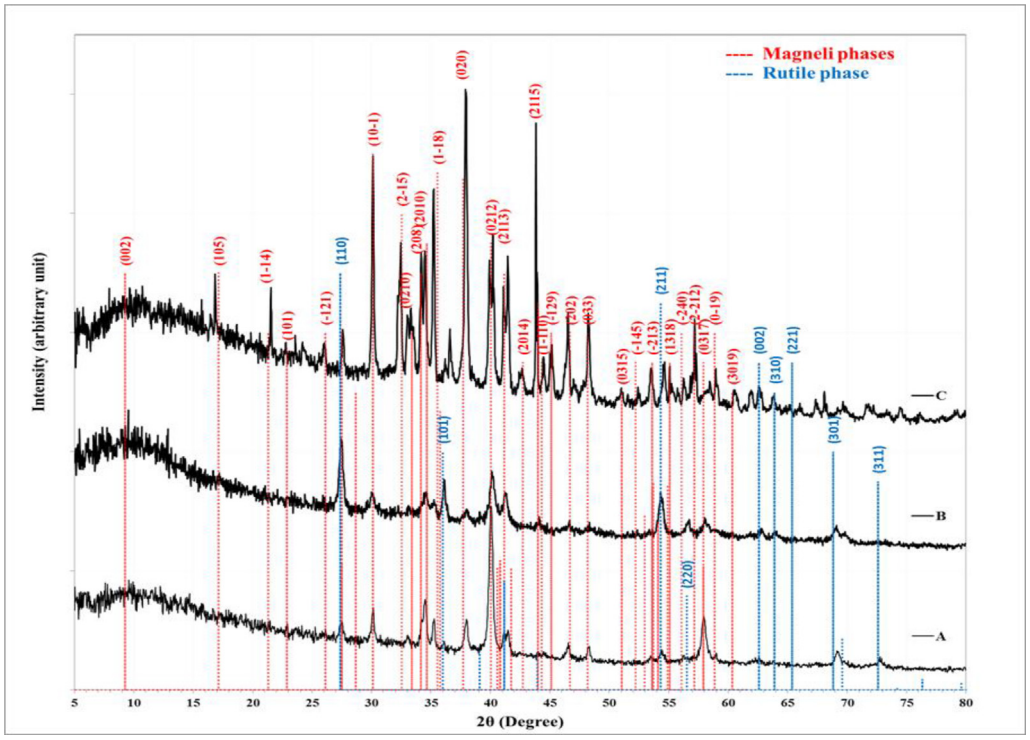

Fig. 3. XRD pattern for the TiO_2 NPs after restructured by hydrothermal at 90 °C for 6 h using different cells diameters of (A) 55 mm, (B) 65 mm and (C) 75 mm.

consistent with the JCPDS card number: 96-100-8196. Notably, the diffractograms of the products of reactors A and B contain peaks related to the crystal planes of the rutile and Magnéli phases, while that of reactor C contains peaks related to a Magnéli phase only. Thus, the production of sub-oxide titanium with the Magneli phase was specific to autoclave reactor C. The phase was confirmed by Raman spectroscopy.

The different surface areas of the reactors resulted in different crystal sizes of their products. It is believed that the difference in the surface area of the reactors is the reason for the growth of a new phase of the product of reactor C due to the increase in the speed of movement of suspended particles during the reaction inside the reactor by increasing the surface area of the liquid. Moreover, applying heat and pressure to the titanium suspension in the reactors caused the formation of titanium and oxygen imbalance ratios, resulting in the formation of the different phases. . Modelling and synthesis of Magnéli phases in ordered titanium oxide nanotubes with preserved morphology.

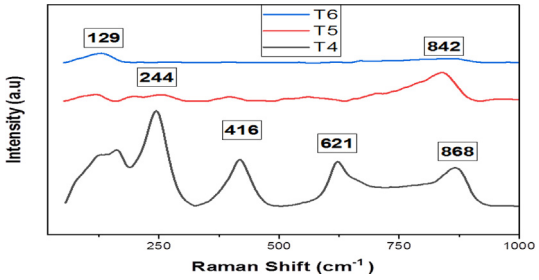

Fig. 4. Raman scattering for the TiO_2 NPs after restructured by hydrothermal at 90 ^{O}C for 6 h using different cells diameters of (T4) 55 mm, (T5) 65 mm and (T6) 75 mm.

Stabilized Magnéli phases are materials characterized by high corrosion resistance in acidic and basic solutions. They possess high electrical conductivity and electrochemical stability [24].

A comparison of the Raman spectra of rutile titanium dioxide with those of the samples from the three reactors revealed that the reaction product in reactor A (T4) had prominent Raman lines at 244, 416, and 621 cm^{-1}, comparable to those of the rutile phase, as illustrated in Fig. 4. All the Raman lines were identical to the rutile stripes except for the one

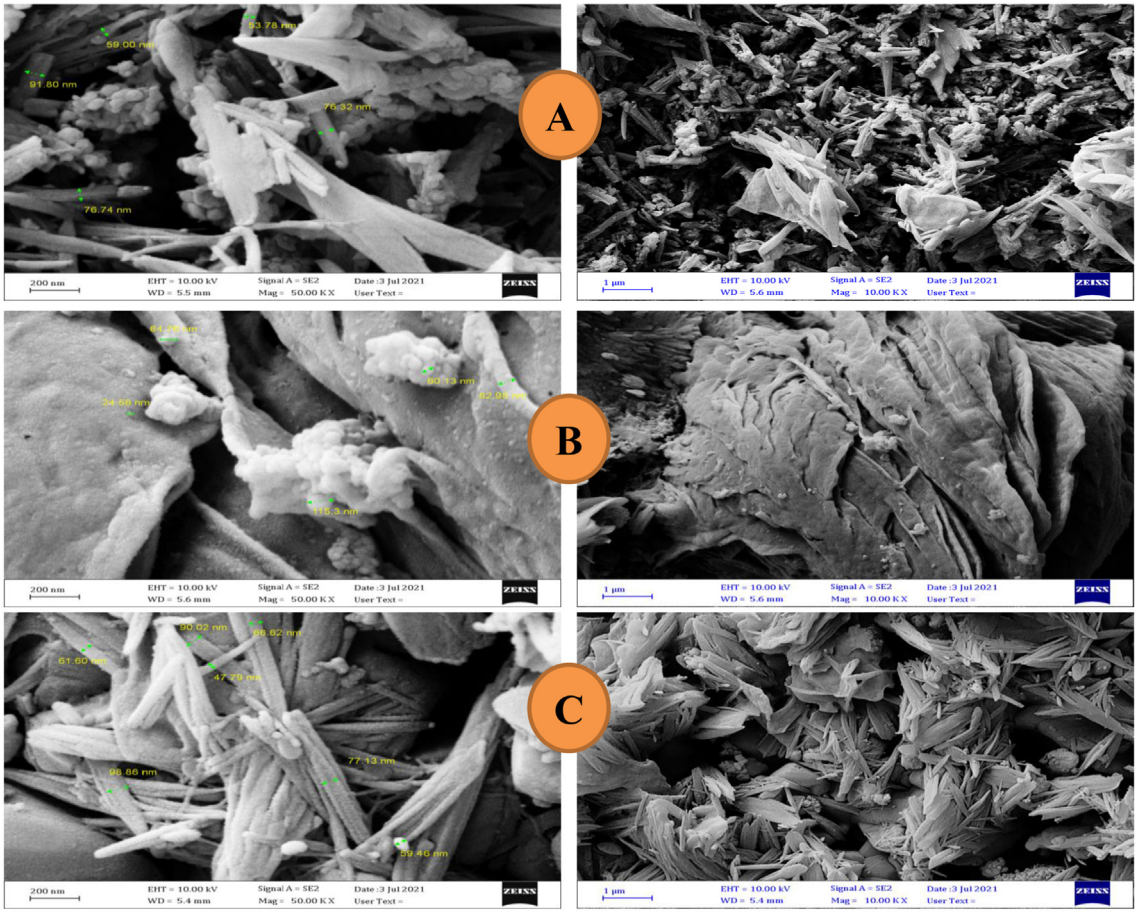

Fig. 5. FE- SEM images two size of the ending result prepared by hydrothermal method using different reactor A, B and C of hierarchical nanostructures.

at 868 cm^{-1}, a result of bending vibration of O–Ti–O in rutile TiO_2. The shift of the position of Raman lines is due to a decrease in the ratio of oxygen, indicating the presence of titanium sub-oxide. Thus, these results confirmed the formation of titanium sub-oxide with the Magnéli phase (Ti_6O_{11} triclinic). Therefore, the dimensions of autoclave reactor C (T6) are optimal for forming Magnéli phase Ti_6O_{11} triclinic.

The absence of these Raman lines in the spectra related to autoclave reactors C (T6) and B (T5) indicates a decrease in the ratios of oxygen bonds with the titanium, which can lead to the formation of the Magneli phase. These results agree with those of Parker and Siegel [25].

The FE-SEM images in Fig. 5 show the topography and morphology of Ti_6O_{11} with the Magnéli phase, the chemical product of the reactions in reactors A, B, and C. They exhibit uniform hierarchical nanostructures with other morphology types, such as planar grass-like shapes.

The products (Ti_6O_{11}) with hierarchical nanostructures have many important applications such as organic degradation, coatings, and supports for the Pt catalysts in solar cells and in various electronic and optoelectronic devices. Titanium suboxides are expected to become important materials in the future [10] because of their excellent conductivity and excellent absorption of visible light. Hierarchical Ti_6O_{11} nanostructures are also very important in various applications because of their huge surface area to volume ratio [26,27].

The minimum crystal size of the products was 53, 24, and 47 nm for reactors A, B, and C, respectively, as clearly observed in the FE-SEM images in Fig. 5., its clearly observed by FE-SEM in Fig. 5.

4. Conclusions

The varying dimensions or surface areas of the reactors resulted in different heat distributions and pressures inside the reactors, causing varied reaction products. Sub-oxide titanium, Ti_6O_{11}, with a Magnéli phase exhibiting hierarchical nanostructures, was formed in reactor C as a result of the reformation of oxygen bonds (Ti–O) of rutile TiO_2 in the reactor. The innovative approach led to producing a Magnéli phase using a hydrothermal method at a low temperature (90 °C). In contrast, other methods require high temperatures (1000 °C) to form the phase.

Conflicts of interest

There is no conflict of interest.

References

[1] S. Andersson, B. Collén, U. Kuylenstierna, A. Magnéli, Phase analysis studies on the titanium-oxygen system, Acta Chem Scand 11 (10) (1957) 1641–1652.

[2] S. Andersson, B. Collen, G. Kruuse, U. Kuylenstierna, A. Magneli, H. Pestmalis, S. Åsbrink, Identification of titanium oxides by X-ray powder patterns. Acta Chemica Scandinavica (Denmark) Divided into, Acta Chem Scand, Ser A and Ser B 1 (1957) 11.

[3] F. Walsh, R. Wills, The continuing development of Magnéli phase titanium sub-oxides and Ebonex® electrodes, Electrochim Acta 55 (22) (2010) 6342–6351. Sep 1.

[4] R. Dinnebier, S. Billinge, eds., Powder diffraction: theory and practice, Royal Society of Chemistry. 2008.

[5] S. Tominaka, Y. Tsujimoto, Y. Matsushita, K. Yamaura, Synthesis of nanostructured reduced titanium oxide: crystal structure transformation maintaining nanomorphology, Angew Chem 123 (32) (2011) 7556–7559. Aug 1.

[6] D. Portehault, V. Maneeratana, C. Candolfi, N. Oeschler, I. Veremchuk, Y. Grin, C. Sanchez, M. Antonietti, Facile general route toward tunable magnéli nanostructures and their use as thermoelectric metal oxide/carbon nanocomposites, ACS Nano 5 (11) (2011) 9052–9061, 22.

[7] E. Khorashadizade, S. Mohajernia, S. Hejazi, H. Mehdipour, N. Naseri, O. Moradlou, A. Moshfegh, P. Schmuki, Intrinsically Ru-doped suboxide TiO2 nanotubes for enhanced photoelectrocatalytic H2 generation, J Phys Chem C 125 (11) (2021) 6116–6127.

[8] A. Arif, R. Balgis, T. Ogi, F. Iskandar, A. Kinoshita, K. Nakamura, K. Okuyama, Highly conductive nano-sized Magnéli phases titanium oxide (TiOx), Sci Rep 7 (1) (2017) 1–9. Jun 16.

[9] R. Tu, G. Huo, T. Kimura, T. Goto, Preparation of Magnéli phases of Ti27O52 and Ti_6O_{11} films by laser chemical vapor deposition, Thin Solid Films 518 (23) (2010) 6927–6932. Sep 30.

[10] X. Baoqiang, S.Y. Hong, M. Yousef, L. Yuanpei, Structures, preparation and applications of titanium suboxides, RSC Adv 6 (83) (2016) 79706–79722.

[11] Z. Zhang, J. Li, X. Wang, J. Qin, W. Shi, Y. Liu, H. Gao, Y. Mao, Growth of Zr/N-codoped TiO2 nanorod arrays for enhanced photovoltaic performance of perovskite solar cells, RSC Adv 7 (22) (2017) 13325–13330.

[12] H. Yin, Y. Wada, T. Kitamura, S. Kambe, S. Murasawa, H. Mori, T. Sakata, S. Yanagida, Hydrothermal synthesis of nanosized anatase and rutile TiO2 using amorphous phase TiO2, J Mater Chem 11 (6) (2001) 1694–1703.

[13] Z. Tan, K. Sato, S. Takami, C. Numako, M. Umetsu, K. Soga, M. Nakayama, R. Sasaki, T. Tanaka, C. Ogino, A. Kondo, Particle size for photocatalytic activity of anatase TiO2 nanosheets with highly exposed {001} facets, RSC Adv 3 (42) (2013) 19268–19271. Oct 8.

[14] Z. Zhang, C. Wang, R. Zakaria, J. Ying, Role of particle size in nanocrystalline TiO2-based photocatalysts, J Phys Chem B 102 (52) (1998) 10871–10878. Dec 24.

[15] Y. Hu, H. Tsai, C. Huang, Effect of brookite phase on the anatase–rutile transition in titania nanoparticles, J Eur Ceram Soc 23 (5) (2003) 691–696. Apr 1.

[16] G. Wilson, A. Matijasevich, D. Mitchell, J. Schulz, G. Will, Modification of TiO2 for enhanced surface properties: finite Ostwald ripening by a microwave hydrothermal process, Langmuir 22 (5) (2006) 2016–2027, 28.

[17] A. Selman, Z. Hassan, Growth and characterization of rutile TiO2 nanorods on various substrates with fabricated fast-response metal–semiconductor–metal UV detector based on Si substrate, Superlattice Microst 83 (2015) 549–564. Jul 1.

[18] T. Vu, H. Au, L. Tran, T. Nguyen, T. Tran, M. Pham, M. Do, D. Nguyen, Synthesis of titanium dioxide nanotubes via one-

step dynamic hydrothermal process, J Mater Sci 49 (16) (2014) 5617–5625.
[19] H. Harada, T. Ueda, Photocatalytic activity of ultra-fine rutile in methanol-water solution and dependence of activity on particle size, Chem Phys Lett 106 (3) (1984) 229–231, 20.
[20] G. Scamarcio, M. Lugará, D. Manno, Size-dependent lattice contraction in CdS 1− x Se x nanocrystals embedded in glass observed by Raman scattering, Phys Rev B 45 (23) (1992) 13792. Jun 15.
[21] C. Xu, P. Zhang, L. Yan, Blue shift of Raman peak from coated TiO2 nanoparticles, J Raman Spectrosc 32 (2001) 862–865.
[22] I. Campbell, P. Fauchet, The effects of microcrystal size and shape on the one phonon Raman spectra of crystalline semiconductors, Solid State Commun 58 (10) (1986) 739–741. Jun 1.
[23] A. De Paula, L. Barbosa, C. Cruz, O. Alves, J. Sanjurjo, C. Cesar, Size effects on the phonon spectra of quantum dots in CdTe-doped glasses, Appl Phys Lett 69 (3) (1996) 357–359. Jul 15.
[24] L. Liborio, N. Harrison, Thermodynamics of oxygen defective Magnéli phases in rutile: a first-principles study, Phys Rev B 77 (10) (2008) 104. Mar 7.
[25] J.C. Parker, R.W. Siegel, Calibration of the Raman spectrum to the oxygen stoichiometry of nanophase TiO2, Appl Phys Lett 57 (9) (1990) 943–945. Aug 27.
[26] X. Li, Y. Liu, J. Ye, Investigation of fabrication of Ti4O7 by carbothermal reduction in argon atmosphere and vacuum, J Mater Sci: Mater Electr 27 (4) (2016) 3683–3692.
[27] S. Andersson, B. Collén, U. Kuylenstierna, A. Magnéli, Phase analysis studies on the titanium-oxygen system, Acta Chem Scand 11 (10) (1957) 1641–1652.